Investigation of the Validity of Miner's Law for Asphalt Mixes

C. Weise
Institute of Pavement Engineering, Dresden University of Technology, Germany

ABSTRACT: Within the analytical pavement design process, Miner's law is used for linear damage accumulation. The aim of the described research project was to investigate the validity of Miner's law especially for asphalt mixes. The investigations were carried out using the cyclic indirect tensile test according to AL Sp-Asphalt 09. The macro-crack formation based on the energy ratio was defined as fatigue criterion. Tests with five different load configurations (with increasing, decreasing, varying and cyclic loading) at five test temperatures have been carried out to investigate the validity of Miner's law. The results show a clear dependency of the damage sum on loading sequence and test temperature. That indicates that Miner's law is not valid for asphalt mixes under the given test conditions. Real loading sequences can't be taken into account. But under consideration of a real temperature distribution in combination with the damage sums obtained in the tests a good conformity with Miner's law can be observed.

KEY WORDS: Miner's law, fatigue life, asphalt mixes.

1 PURPOSE OF THE STUDY

Various stresses occur in asphalt pavements as a result of traffic loading and climate impact. Currently, the analytical pavement design process of asphalt pavements is performed regarding the fatigue state at the lower surface of the asphalt base layer and under consideration of the material properties of the used mixes. So it becomes possible to optimize the pavement layers. Within the design process, the damages caused by the numerous load states are added linearly using Miner's law. Miner's law has been developed on the basis of uniaxial tensile tests on aluminium samples. That is the reason why the validity of Miner's law must be verified for asphalt mixes.

2 INTRODUCTION

2.1 Miner's Law

Miner's law allows the accumulation of different damages. Based on cyclic uniaxial tensile and tensile/compression tests on aluminium samples, Miner formulated the following hypothesis:

$$\sum_i \frac{n_i}{N_i} = 1 \tag{1}$$

wherein n_i = number of load cycles applied at stress i; N_i = number of load cycles to failure at stress i.

Each load cycle consumes a small quantity of the material's lifetime. According to Miner's law, the chronological order of the damage does not influence the damage value. In this context, the term endurance limit is used for stresses i where the number of load cycles to failure is infinite, i.e. no damage occurs. The endurance limit could not be verified for asphalts until now. So it must be assumed that the endurance limit does not exist. Furthermore, Miner did not include the endurance limit in his hypothesis.

It has already been proved for other materials, in particular steel that the independence of the damage from the chronological order postulated in Miner's law does not exist. That means that load cycles with elastic strains below the endurance limit (which exist for steel) causes damage when they occur in combination with load cycles with large elastic strains (Radaj 2007). The endurance limit of steel decreases because of premature damage. In other words, the endurance limit depends on the load order.

The tests Miner conducted on aluminium samples already showed large variances of the summation of the different damage portions. The damage sum for the test results published varies between 0.60 and 1.49 (Miner 1945). Miner used the fracture of the sample as damage criterion. Nevertheless, Miner's law is used within the analytical pavement design process.

2.2 Nonlinear Damage Accumulation

As a rule, nonlinear damage development occurs in technical materials and components. If the damage portion n_i/N_i depends on the stress amplitude, nonlinear damage accumulation becomes the criterion. Equation 2 gives an example of a nonlinear damage process.

$$\sum_i \left(\frac{n_i}{N_i}\right)^p = 1 \tag{2}$$

It must be clarified if this constraint is also valid for asphalt, which means that the damage speed increases with an increasing stress amplitude.

The actual damage that occurs during the test can only be determined using the curve of the elastic strain related to the elastic strain at the moment of macro-cracking (fatigue criterion, see section 2.3). Figure 1 shows the curves of the weighted elastic strain for three different strain amplitudes caused by three loading amplitudes. The diagram shows that there is no difference in the damage speed. Hence, asphalt has linear damage behaviour.

2.3 Evaluation of Fatigue Tests

Different fatigue criteria can be used for the evaluation of fatigue tests. For the described tests (cyclic indirect tensile tests, see section 3.1), the method of energy ratio ER based on the concept of dissipated energy (Hopman 1993) has been used to determine the moment of macro-crack formation. For harmonic periodical stresses, the dissipated energy during one load cycle can be calculated using equation 3.

$$W_i = \pi \cdot \sigma_i \cdot \varepsilon_i \cdot \sin \varphi_i \tag{3}$$

wherein W_i = dissipated energy; σ_i = maximum stress; ε_i = elastic strain; φ_i = phase angle between stress and strain

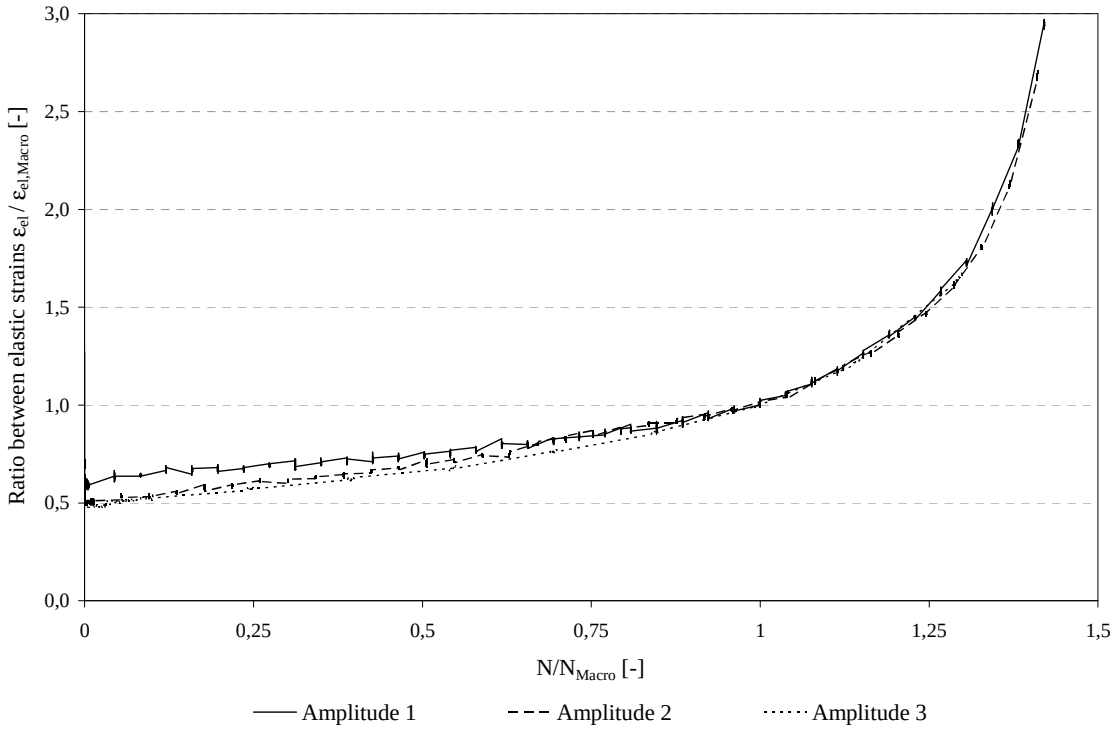

Figure 1: Weighted elastic strain curve for different loading amplitudes

The energy ratio ER relates the dissipated energy of load cycle i to the dissipated energy of the initial state 0 and can be calculated using equation 4.

$$ER(N_i) = \frac{N_i \cdot W_0}{W_i} = \frac{N_i \cdot (\pi \cdot \sigma_0 \cdot \varepsilon_0 \cdot \sin\varphi_0)}{\pi \cdot \sigma_i \cdot \varepsilon_i \cdot \sin\varphi_i} \tag{4}$$

wherein N = number of load cycles; W = dissipated energy; σ = maximum stress; ε = elastic strain; φ = phase angle between stress and strain

Assuming that during the test the induced stress and also the phase angle are constant ($\sigma_0 = \sigma_i$; $\varphi_i = const.$) and $\varepsilon = \sigma/E$, equation 4 can be simplified.

$$ER(N_i) = N_i \cdot E_i \tag{5}$$

wherein N_i = number of load cycle; E_i = stiffness modulus

Fatigue functions can be arranged on the basis of stress or strain. This research project studies strain-based fatigue functions.

3 LABORATORY TESTS

Cyclic indirect tensile tests (CITT) are conducted to examine the validity of Miner's law for asphalt mixes: one the one hand, these were tests with constant stress amplitudes and, on the other, tests with five different loading configurations. The tests and the test conditions are specified in the following sections.

3.1 Cyclic Indirect Tensile Test (CITT)

In CITTs, a circular disk specimen is loaded diametrically between two loading strips (see Figure 2). Because of the specimen shape and the linear transmission of force to the lateral area, an inhomogeneous state of stress occurs in vertical and horizontal directions. FEM calculations verify that the horizontal tensile stress in the middle of the specimen is nearly constant over approximately 70% of the specimen's diameter. In the area of force transfer, horizontal compressive stresses appear. The mean value of the vertical compressive stress is located in the middle of the specimen and the maximum value in the area of load transfer. In the centre of the specimen, the ratio between vertical compressive stress and horizontal tensile stress is 3 to 1.

The dimensions of the samples are chosen as a function of the maximum grain size. For a maximum grain size of 11 mm, the specimen diameter should be 100 mm and the height 40 mm. The loading strips had a width of 12.7 mm (AL Sp-Asphalt 09).

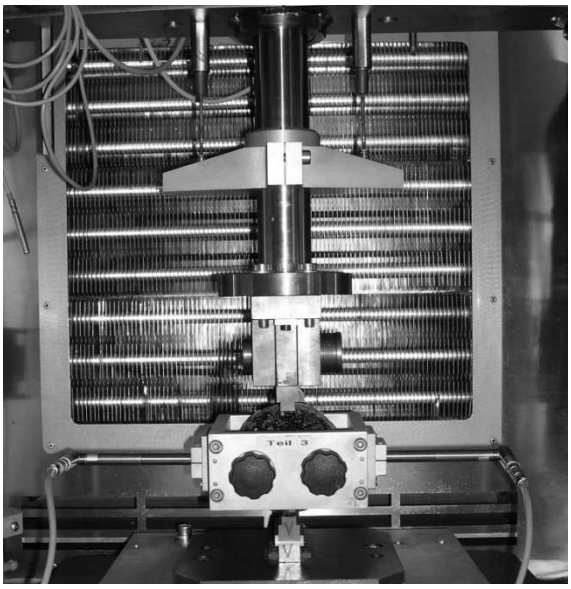

Figure 2: Principle of the cyclic indirect tensile test

3.2 Asphalt Mixes investigated and Sample Preparation

Stone mastic asphalt with a maximum grain size of 11 mm and 6.5% polymer modified bitumen (SMA 11 S 25/55-55A) was used for the tests. The air void content of the samples was between 2.69 and 3.77 Vol.-%. This corresponds to a bulk density variance of 0.03 g/cm³. The asphalt was produced in a mixing plant. The asphalt slabs were fabricated in the laboratory using a segmented roller compactor and a deformation-controlled compaction regime. Afterwards, specimens were drilled out of the slabs and the air void content as well as the dimensions were determined for each specimen.

3.3 Test Conditions and Load Configuration

The CITTs have been carried out at 5 Hz to ensure maximum accuracy with regard to the test procedure. Due to the limited space the results concerning different frequencies are not described in this paper. The chosen test temperatures are -10, -2.5, 5, 12.5 and 20 °C. They are evenly spread over the possible temperature range of the CITT. The load, which was applied

to the specimen, had the form of a harmonic sinusoidal wave without any rest periods. The wave is defined by lower and upper stress. Depending on the test temperature, the cryogenic stress or the necessary contact stress have been chosen as lower stress value. For the determination of fatigue functions, the upper stress has been varied three times. Table 1 gives a summary of the chosen stress values.

Table 1: Test conditions for CITTs

temperature T [°C]	lower stress σ_U [N/mm²]	upper stress		
		$\sigma_{O;1}$ [N/mm²]	$\sigma_{O;2}$ [N/mm²]	$\sigma_{O;3}$ [N/mm²]
-10	0.845	1.60	1.80	2.200
-2.5	0.312	1.20	1.40	1.700
5	0.106	0.85	1.00	1.223
12.5	0.051	0.50	0.70	0.900
20	0.035*	0.30	0.45	0.600

* necessary contact stress

Fatigue tests with constant stress amplitudes according to AL Sp-Asphalt 09 have been carried out (triple repeated) and evaluated and formed the basis for the following tests to verify Miner's law. Tests with five different load configurations were conducted to prove the validity of Miner's law. Figure 3 illustrates the chronological order of the different load levels. The duration of each load level depends on the test temperature. The load configurations can be described as:

- configuration A: increasing loading
- configuration B: decreasing loading
- configuration C: varying loading
- configuration D: cyclic loading

Load configuration D was tested in two versions. In version D50, each loading level has a length of 50 load cycles. In version D500 however, each load level has a duration of 500 load cycles. The lengths of the load levels 1 (low), 2 (medium) and 3 (high) for load configurations A, B and C are given in Table 2. They were derived from the results of the fatigue tests with constant stress amplitudes. To ensure that the macro-crack occur during the test the last load level was extended. I.e. load level 1 at load configuration A has not the same length than load level 1 at load configuration B.

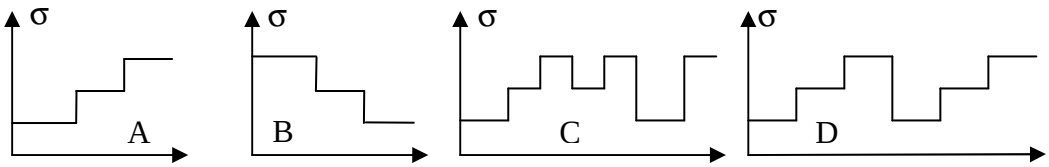

Figure 3: Load configurations

3.4 Evaluation of Tests

The maximum value of the curve of the Energy Ratio can be interpreted as the moment of macro-crack formation. The maximum can be identified using a polynomial of degree six. Evaluating the fatigue tests with constant stress amplitudes produces strain-based fatigue functions. The fatigue functions are generated for each test temperature to ensure maximum accuracy. Figure 4 shows the five fatigue functions. These results are used to determine the lengths of the different load levels (see Table 2) and the number of load cycles N_i until failure at stress i.

Table 2: Scheduled load levels lengths (number of cycles) for load configurations A, B and C depending on the test temperature

T [°C]	load level	load configuration A	load configuration B	load configuration C
-10	1	30,000	60,000	10,000
	2	10,000	10,000	5,000
	3	6,000	2,000	1,000
-2.5	1	15,000	50,000	7,500
	2	6,000	6,000	3,000
	3	5,000	1,000	500
5	1	10,000	30,000	5,000
	2	4,000	2,000	2,000
	3	16,000	1,000	1,000
12.5	1	22,000	50,000	11,000
	2	3,500	3,500	1,750
	3	5,000	1,000	500
20	1	15,000	50,000	5,000
	2	3,000	3,000	2,000
	3	10,000	1,250	1,000

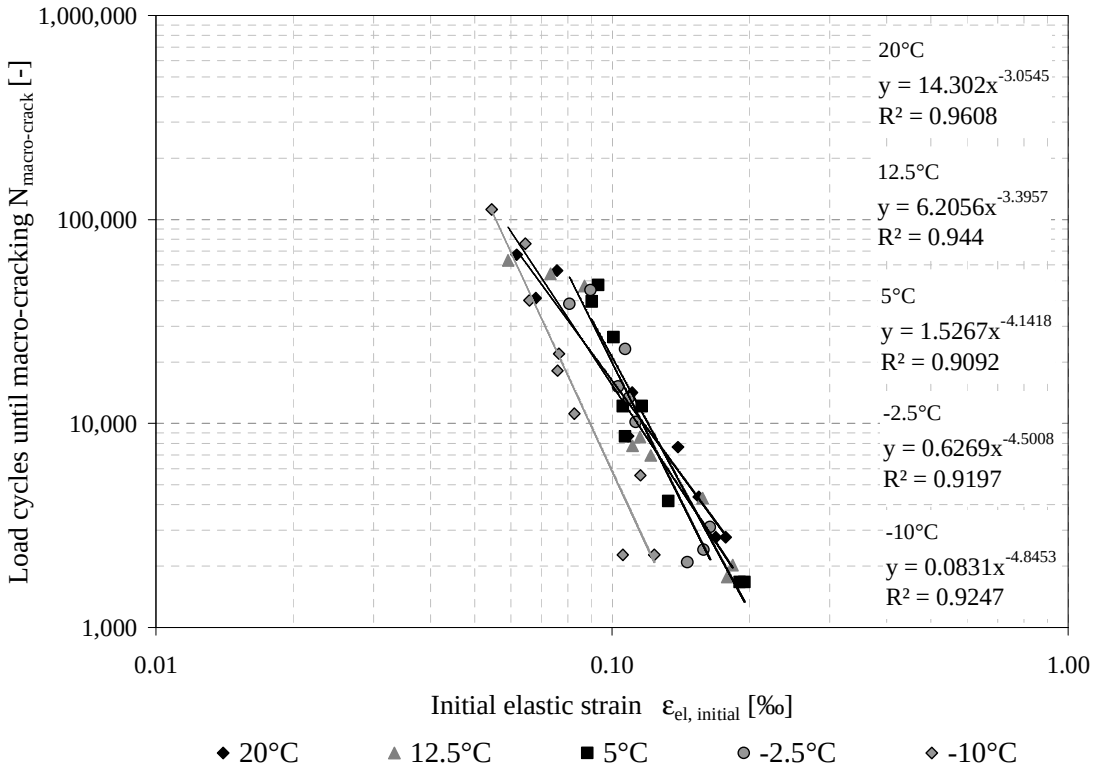

Figure 4: Fatigue functions for the different test temperatures (constant stress amplitudes)

At the beginning of each test with the varying loading configurations, a pre-test of three times 50 load cycles was performed to determine the initial elastic strain of each load level. Thanks to this procedure, the number of load cycles until failure can be investigated. Directly after the pre-test, the intended loading configuration was applied to the specimen. Figure 5 illustrates the curve of the energy ratio ER for a test conducted at 12.5 °C and loading configuration D500. Points of discontinuity can be observed in the diagram because of the simplified assumption of the energy ratio in Equation 5 and the minor impact of the stress amplitude on the stiffness modulus.

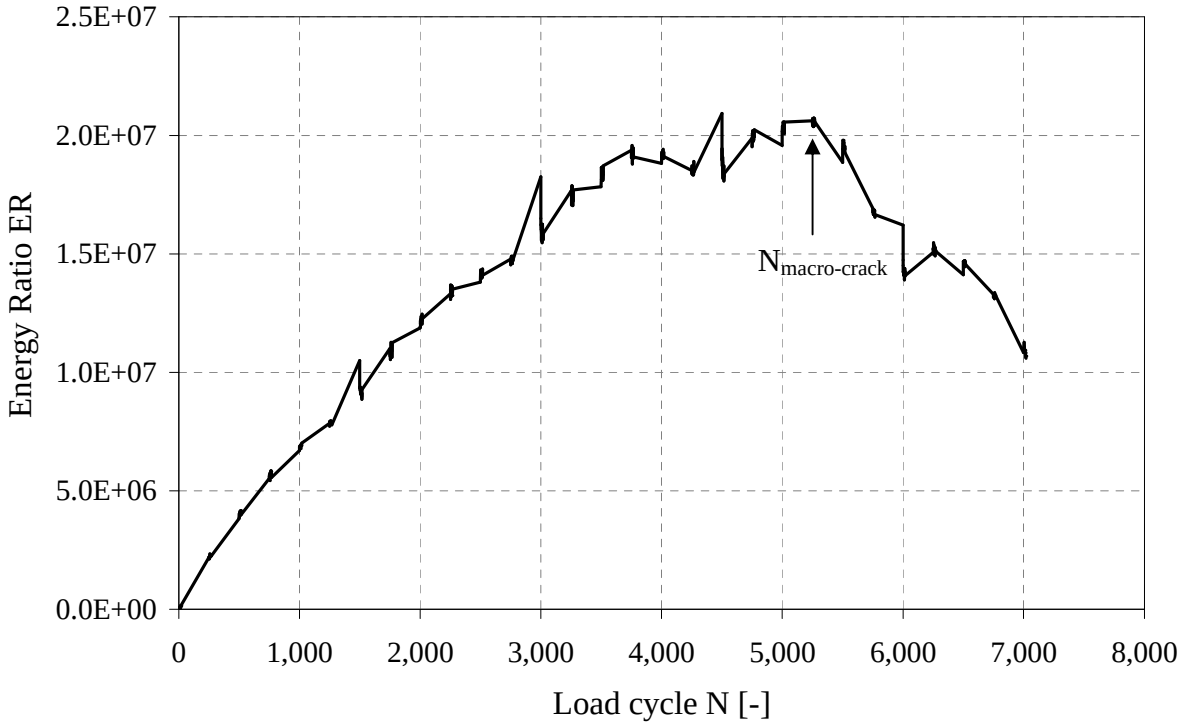

Figure 5: Curve of the energy ratio ER (12.5 °C, D500)

4 TEST RESULTS

4.1 Impact of the Loading Sequence

The damage sum of the different loading configurations in Figure 6 shows a clear dependence on the loading configuration and the load order, respectively. The following findings can be derived from the test results:

(1) The damage sum is lower for increasing loading compared with decreasing loading (difference between configuration A and B). That means that a high initial loading does not lead to early failure.

(2) The length of each load level has an important impact on the damage sum. Fast changes in the load level, as it occurs in situ, lead to a lower damage sum (difference between configuration D500 and D50).

It seems to be impossible to derive the dependence of the damage sum from the loading configuration using the test results because random loading configurations occur in situ. Furthermore, recovery, which has a positive effect on the damage sum, cannot be taken into account. Recovery is caused, for example, by rest periods of different lengths. The study of this effect would require real time tests. Furthermore, the scatter of the test results (on the one hand, the number of load cycles until failure and the damage sum, on the other) is really high. It could be observed that the scatter is especially high for low test temperatures and for loading configurations with varying and cyclic loading. In Figure 6, the minimum and maximum of the damage sum for 5 °C are also given.

A damage sum above 1 means, that the specimens tolerate more load cycles until failure than predicted using the fatigue functions. This causes a larger safety if the fatigue function is used i.e. for the pavement design process.

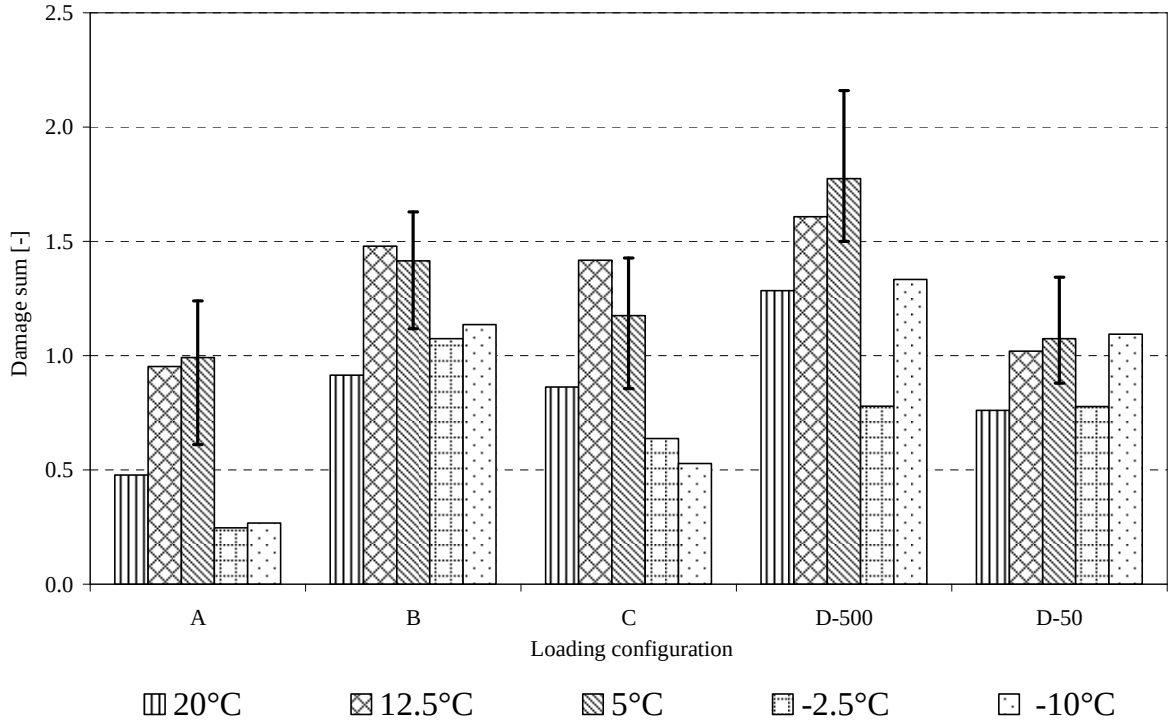

Figure 6: Impact of loading configuration on the damage sum and the range for 5 °C

4.2 Impact of the Test Temperature

Figure 7 shows the temperature-dependent average values of the damage sum for the five loading configurations. Without considering the loading configuration, the average value of the damage sum is nonlinear over the test temperature. The minimum and maximum values caused by different loading configurations are also given in Figure 7. The average value of the damage sum is larger than 1.0 for test temperatures 5 and 12.5 °C. For the other temperatures, the values are below 1.0. If you calculate the average over the given values again, you obtain 1.002 which is the failure criterion postulated by Miner. This approach assumes that Miner's law is valid for asphalt mixes under the given conditions.

It must be taken into account that temperatures within an asphalt pavement did not appear at the same frequency. Figure 8 gives the temperature distribution of the surface temperature for the station Dresden Airport using measurements made between 1991 and 2005. The temperature levels are divided into 5 °K intervals and characterised by the mean value. The first step was to calculate the frequencies of the temperature levels -10, 5 and 20 °C using the characteristic values of the two neighbouring values. Because the sum of the frequencies of the five test temperatures is only 52.5% the frequencies have to be reweighted. So the sum over the frequencies is 100%. By linking the determined temperature frequencies $h(T)$ with the damage sum $n_i/N_i(T)$ and adding all single terms we obtain 1.07 (see equation 6). The result indicates that the used temperature distributions obviously lead to a compensation of the high and low parts of the damage sum. In order to confirm this result, more temperature distributions must be investigated.

$$\sum h(T) \times \frac{n_i}{N_i} = 0.315 \cdot 0.872 + 0.1794 \cdot 0.703 + 0.3044 \cdot 1.286 + 0.2519 \cdot 1.295 + 0.2328 \cdot 0.854 = 1.07$$

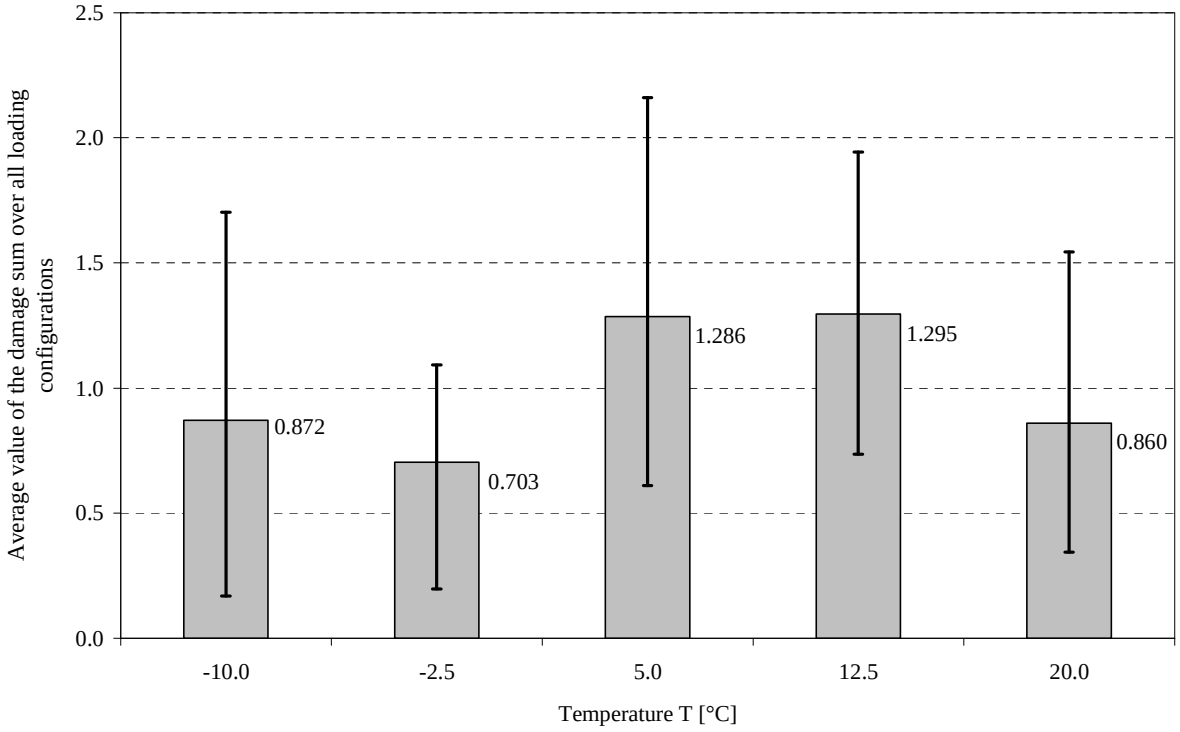

Figure 7: Impact of test temperature on damage sum (average over all load configurations)

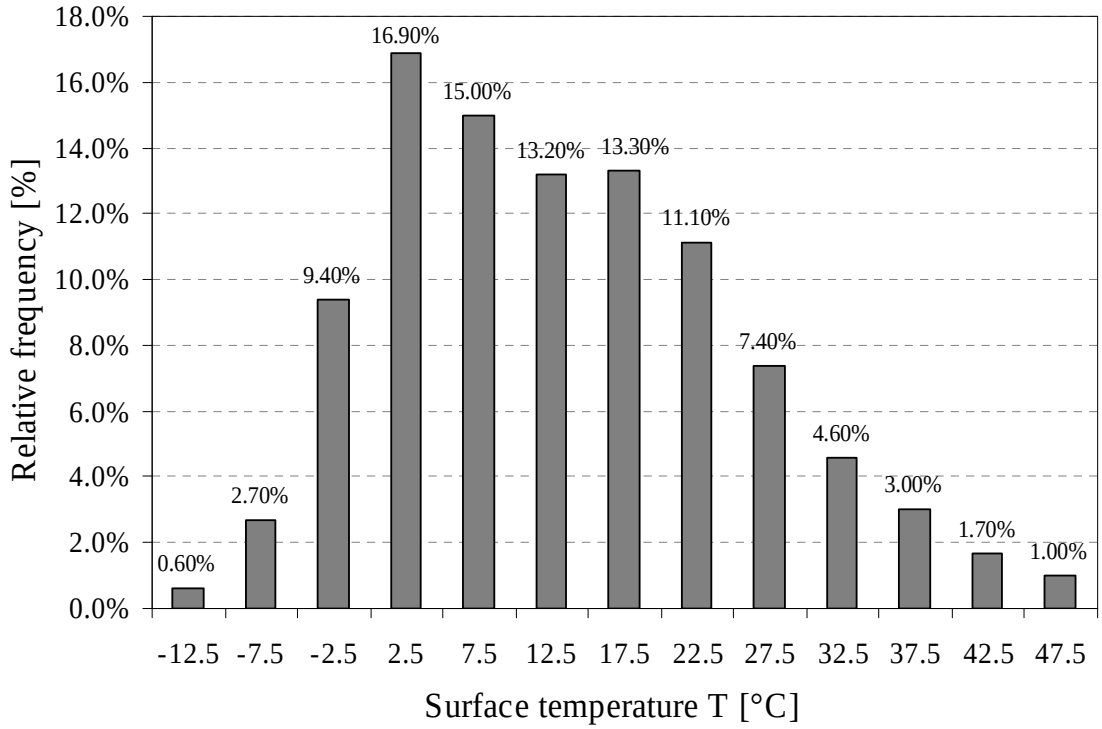

Figure 8: Frequency distribution of the surface temperature (station: Dresden-Klotzsche, 1991-2005) (Kayser 2007)

5 CONCLUSION

Considering the test results of the CITTs and the test conditions, the validity of a hypothesis of linear damage accumulation can be confirmed. The investigation of five different loading configurations at five test temperatures shows a clear impact of the load order and the test temperature on the damage sum at failure. The impact of the test temperature is of particular importance because the loading sequence cannot be taken into account especially with regard to the impact of rest periods. It is not possible to determine this effect using accelerated tests. The damage sum obtained on the basis of the test results in combination with a real temperature distribution is 1.07. The CITT and also other fatigue tests can be conducted at a maximum test temperature of 20 °C. Hence, the impact of higher temperatures on the damage sum can only be presumed. It seems to be realistic that the obtainable damage sum at these temperatures does not increase compared with the value of 20 °C.

The test results published by Miner already showed a large scatter which can be confirmed by the current test results. From this follows, that the use of statistic methods is required. In the future, it will be possible to consider different security levels by using cumulative frequency curves.

ACKNOWLEDGEMENT

The author gratefully acknowledges the financial support of the DFG – German Research Foundation (Deutsche Forschungsgemeinschaft).

REFERENCES

AL Sp-Asphalt 09, 2009. Test methods for the design of asphalt pavements: Method for the determination of the stiffness and fatigue characteristics of bituminous mixes using the indirect tensile test (in German). Forschungsgesellschaft für Straßen- und Verkehrswesen, Köln, Germany.

Radaj, D.; Vormwald, M., 2007. *Fatigue strength (Ermüdungsfestigkeit - Grundlagen für Ingenieure)*. Springer-Verlag, Berlin, Germany.

Kayser, S., 2007. Principles for survey of climatic influences within the flexible pavement design process (Grundlagen zur Erfassung klimatischer Einflüsse für Dimensionierungsrechnungen von Asphaltbefestigungen). PhD thesis, University of Technology Dresden, Germany.

Miner, M. A., 1945. *Cumulative damage in fatigue*. Journal of Applied Mechanics, Vol. 12, Issue 3.

Hopman, P.; Kunst, P. & Pronk, A., 1989. *A Renewed Interpretation Model for Fatigue Measurement. Verification of Miner's Rule*. 4th Eurobitume Symposium, 4-6 October 1989, Vol. 1, pp. 557-561, Madrid, Spain.